Available online at www.sciencedirect.com
SCIENCE DIRECT
Polymer 46 (2005) 8239–8249
polymer
www.elsevier.com/locate/polymer

Free volume sizes in intercalated polyamide 6/clay nanocomposites

Petra Winberg[a], Morten Eldrup[a,b], Niels Jørgen Pedersen[b], Martin A. van Es[c], Frans H.J. Maurer[a,*]

[a]*Department of Polymer Science and Engineering, Lund Institute of Technology, Center for Chemistry and Chemical Engineering, Lund University, SE-221 00 Lund, Sweden*
[b]*Materials Research Department, Risø National Laboratory, DK-4000 Roskilde, Denmark*
[c]*Research and Development DSM Dyneema, Urmond, The Netherlands*

Received 12 April 2005; received in revised form 14 June 2005; accepted 22 June 2005
Available online 19 July 2005

Abstract

The effect of incorporating modified clay into a polyamide 6 (PA6) matrix, on the free volume cavity sizes and the thermal and viscoelastic properties of the resulting nanocomposite, was studied with positron annihilation lifetime spectroscopy, differential scanning calorimetry and dynamic mechanical analysis. At low concentrations of clay the fraction of PA6 crystals melting close to 212 °C was increased, while the fraction of the α-form PA6 crystals, melting close to 222 °C, was reduced. At higher concentrations of clay, a crystal phase with increased thermal stability emerged. Addition of more than 19 wt% clay caused a reduction of the heat of fusion of PA6. An unexpected reduction of the ΔC_p at the glass transition, contradicting the measured reduction of the heat of fusion, was detected, indicating an altered mobility in the non-crystalline regions. The viscoelastic response of PA6/clay nanocomposites, as compared to unfilled PA6, pointed towards a changed mobility in the non-crystalline regions. At high concentrations of clay (>19 wt%) an increase of the free volume cavity diameter was observed, indicating a lower chain packing efficiency in the PA6/clay nanocomposites. The increased free volume sizes were present both above and below the glass transition temperature of PA6.

Keywords: Silicate; Positron annihilation; Free volume

1. Introduction

Recently there has been an increased interest in the physical behavior of polymers in confined environments and of polymers in close contact with surfaces. The behavior of polymers under these conditions is of great importance in many fields of technology such as polymer composites and blends, and in applications such as biomedical implants, electronics, adhesives and lubricants. Many studies of confinement and surface effects on polymers have been focused on layered silicates dispersed in a polymer matrix, often referred to as polymer clay nanocomposites [1–6]. Depending on the preparation method and the properties of the components, two main types of polymer clay nanocomposite structures can be achieved. An intercalated structure is obtained when polymer chains are able to intercalate and expand the distance between the silicate layers, while an exfoliated structure is obtained when the silicate layers are fully separated and dispersed in the polymer matrix.

A large influence of layered silicates on the crystalline structure and crystallization kinetics in polymers has been observed for a number of different polymer/clay systems [7–16]. The changes in crystalline structure and crystallization kinetics have been ascribed to the small distance between the silicate layers which hinders the crystal growth, as well as to the confinement of chains in between the silicate surfaces in intercalated nanocomposites [11,12] and to surface interactions [10,11]. In polyamide 6 (PA6), layered silicates have been shown to alter the crystalline structure by favoring the formation of pseudohexagonal γ-form crystals, which have a lower packing density as compared to the α-form crystal, which is the primary crystalline form in unfilled PA6 [7,8,10,11,13,14]. The crystallization kinetics of PA6 is influenced by the clay content and by the interaction between the clay and the polymer. In addition,

* Corresponding author. Tel.: +46 46 222 9149; fax: +46 46 222 4115.
E-mail address: frans.maurer@polymer.lth.se (F.H.J. Maurer).

0032-3861/$ - see front matter © 2005 Elsevier Ltd. All rights reserved.
doi:10.1016/j.polymer.2005.06.063

the crystal structure of PA6 undergoes a phase transition when subjected to heating and the crystal structure of PA6/layered silicate composites is, therefore, also influenced by processing and thermal treatment [11,13,14,17].

Altered chain dynamics in polymer clay nanocomposites have been observed with a number of different experimental techniques including nuclear magnetic resonance [14,18], dielectric spectroscopy [1,14], quasi-elastic neutron scattering [19] and differential scanning calorimetry [5]. Exfoliated polymer clay nanocomposites have been reported to exhibit longer relaxation times, as compared to bulk PA6, indicative of solid-like behavior [3,5,18]. The increased relaxation times have been ascribed to polymer segments adjacent to the silicate layers experiencing strong interaction with the silicate layers and reduced entropy. In addition to the slower relaxation behavior, enhanced local dynamics much faster than the bulk have been reported for intercalated hybrids with an inter-gallery distance much smaller than the radius of gyration of the polymer. The enhanced dynamics are typically ascribed to confinement induced density inhomogeneities in the inter-gallery region, suggested to be caused by absence of chain entanglements and packing constraints [1,3,14,18]. Fast relaxation of polymer chains confined between clay layers, due to density-inhomogeneities, has been supported by molecular dynamics simulations [20].

Given the observed large effects of clay on chain dynamics and crystalline structure in semi-crystalline polymers and considering the strong interrelations between chain dynamics and free volume in polymers, it would be particularly useful to gain information on the free volume structure in polymer clay nanocomposites. The free volume in a polymer is the space available for segmental motions, such as the large-scale motions associated with the glass transition. The chain dynamics, therefore, depends on the free volume in the system in a wide temperature range [21,22]. Positron annihilation lifetime spectroscopy (PALS) is a technique, which probes the free volume cavities by measuring the lifetime of *ortho*-positronium (*o*-Ps) before annihilation at the free volume sites of the polymer. The lifetime of *o*-Ps is a direct measure of the free volume cavity size. So far, studies on the free volume structure of polymers in close contact with surfaces, which have mainly been focused on thin polymer films [23–26] and polymers filled with nano-sized spherical fillers [27–30], have revealed changes in the free volume sizes as compared to the bulk state. Positron lifetime experiments on polymer clay nanocomposites have been reported for only a few polymer clay systems [31–34]. Intercalated polystyrene/clay composites with a very high clay content (75 wt%) showed a positron annihilation behavior in the nanocomposite very similar to the behavior in the clay itself. Recently, Becker et al. [32] studied the influence of clay on the free volume properties in cured epoxy and found an indication of increased free volume sizes in the polymer due to the presence of clay.

The aim of this study was to investigate whether changes in thermal and viscoelastic behavior of intercalated polyamide 6 (PA6)/organically modified clay composites as compared to the bulk polymer can be correlated to changes in the free volume cavity sizes in the composites. The intercalation of the organically modified clay was measured with small-angle X-ray scattering (SAXS). Changes in thermal and viscoelastic behavior of intercalated PA6/clay composites were measured with differential scanning calorimetry (DSC) and dynamic mechanical analysis (DMA). The free volume cavity sizes in all PA6/clay nanocomposites were measured by means of positron annihilation lifetime spectroscopy (PALS) at ambient conditions. The temperature dependence of the free volume cavity sizes in unfilled PA6, organically modified clay and composite with 35 wt% clay were studied at temperatures between −10 and 150 °C.

2. Experimental

2.1. Materials

Polyamide 6 (PA6), Akulon K123 with a number average molecular weight of 13,000 g/mol was received from DSM Research, the Netherlands, and layered silicate (CloisiteNa$^+$) and organically modified layered silicates (Cloisite20A, Cloisite30B, Cloisite93A) were obtained from Southern Clay Products, USA. The cation exchange capacity of the layered silicates was between 90 and 95 mequiv. The cation in Cloisite20A, Cloisite30B and Cloisite93A was dimethyl dihydrogenated tallow quarternary ammonium ions, methyl tallow bis-2-hydroxyethyl quarternary ammonium ions and methyl dihydrogenated tallow ammonium ions, respectively, which in the following text is referred to as organic modification. The total content organic modifier in Cloisite20A was determined by thermal gravimetric analysis (TGA) to be 38.8 wt%. Based on the exchange capacity of the clay and the molecular mass of the organic modification [35], about 21 wt% of the total content organic modifier is in excess. Nanocomposites were prepared at DSM Research, the Netherlands, by melt mixing cryogenically milled PA6 and Cloisite20A in a W&P ZSK 30 42D co-rotating twin screw extruder operated at 400 rpm [14]. After drying in vacuum at 80 °C for 24 h the melt-mixed composites were compression molded in a press at 250 °C with subsequent cooling to room temperature at approximately 10–5 °C/min while maintaining constant pressure. Samples were stored in a dry environment at room temperature before measurements. Unless stated otherwise, the composites are labeled by the content of organically modified clay. PA6-35 wt% contains 21 wt% silicate and 14 wt% organic modifier. It should also be noted that unless stated otherwise data regarding the physical properties of clay and its organic modifier, as well as its influence on the physical properties of PA6, was obtained

from measurements on Cloisite20A and PA6/Cloisite20A nanocomposites.

2.2. Extraction of organic modifier and preparation of PA6/organic modifier

Organic modifier, reported as dimethyl dihydrogenated tallow quarternary ammonium salt [35] was extracted from Cloisite20A with refluxing ethanol using a soxlet extraction apparatus. The ethanol was evaporated and the remaining extract dried in vacuum at room temperature for 1 h. The dried organic modifier was mixed with PA6 using a DSM Midi 2000 co-rotating twin screw extruder with a chamber capacity of 15 cm^3, at 260 °C and 80 rpm for 10 min. The melt-mixed material, which contained 7 wt% organic modifier, was compression molded immediately after mixing in a press at 250 °C with subsequent cooling to room temperature at approximately 6 °C/min while maintaining constant pressure. Samples were dried in vacuum for 24 h at 80 °C and stored in a dry environment at room temperature before measurements. FTIR spectra of the extracted modifier and Cloisite20A for comparison are shown in Fig. 1.

2.3. Differential scanning calorimetry (DSC)

The thermal properties of the molded materials were studied using a DSC Q1000 from TA Instruments. The samples were contained in hermetic aluminum pans and the analysis was performed under N_2 purge. Glass transition data, T_g and ΔC_p, were recorded during heating at 20 °C/min, while melting data were recorded during heating at both 10 and 20 °C/min. The cooling rate was 10 °C/min. The samples were dried in vacuum at 80 °C for 24 h before measuring. The cell resistance and capacitance was calibrated before the measurements, using empty cells and sapphire disks, in the temperature range between −90 and 400 °C. The heating rate was 20 °C/min. The enthalpy constant and the *x*-axis temperature were calibrated by measuring the melt enthalpy and temperature of indium, using a heating rate of 10 °C/min.

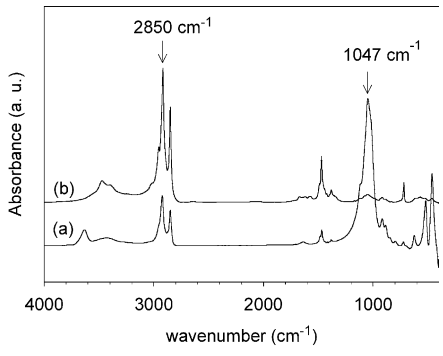

Fig. 1. Infrared absorption spectra of organically modified clay (a) and extracted modifier (b). The Si–O–Si and C–H absorption bands are indicated with arrows at 1047 and 2850 cm^{-1}, respectively.

2.4. Positron annihilation lifetime spectroscopy (PALS)

The free volume structure of the unfilled PA6, clay and the nanocomposites was studied with positron annihilation lifetime spectroscopy (PALS). PALS employs a radioactive material, in this case ^{22}Na encapsulated between sheets of Kapton, which emits positrons during its decay. The encapsulated radioactive material is sandwiched between two pieces of the material, which is under study. When the source emits a positron, a 1.28 MeV gamma ray is simultaneously emitted and the 'birth' of the positron can thus be detected. When the positron annihilates with an electron, two gamma rays of 0.51 MeV are emitted. One of these gamma rays is detected and the lifetime of the positron can thus be measured. The positrons can annihilate directly with an electron, yielding a lifetime (τ_2) of about 0.4 ns, The positrons can also form bound states with an electron from the polymer. *para*-positronium (*p*-Ps), which is the bound state between the positron and an electron with anti-parallel spin, has a lifetime (τ_1) of about 0.125 ns. *ortho*-positronium (*o*-Ps), which is the bound state between the positron and an electron with parallel spin, exhibits a much lower annihilation rate reaching a lifetime of about 142 ns in vacuum. However, in polymers *o*-Ps can annihilate through pick-off of a second electron which shortens its lifetime (τ_3) to about 1–5 ns [36]. It has been shown that *o*-Ps mainly resides in regions with low electron density, which in polymers are the free volume sites, and τ_3 is related to the size of the free volume cavities. The relationship between the *o*-Ps lifetime (τ_3), in ns, and the free volume cavity radius (R) and size (V), is described by a simplified model proposed by Tao [37], which leads to a semi-empirical relationship (1a) and (1b) [38]. The model assumes that the positronium is localized in an infinite spherical potential well with a radius R_0. Assuming an electron layer thickness (ΔR) equal to 0.166 nm [38,39], the mean radius ($R = R_0 - \Delta R$) of the free volume cavities can be calculated. We apply this approximate relationship to estimate the free volume sizes in PA6/clay nanocomposites from PALS measurements.

$$\tau_3 = 0.5\left(1 - \frac{R}{R_0} + \frac{1}{2\pi}\sin\frac{2\pi R}{R_0}\right)^{-1} \quad (1a)$$

$$V(\tau_3) = \frac{4\pi R^3}{3} \quad (1b)$$

The measurements of positron lifetimes in PA6, Cloisite20A and PA6/clay nanocomposites as a function of clay content were performed using a source which gave a count rate of 60–80 s^{-1} and each spectrum consisted of at least 2.5 million counts. While the measurements performed at room temperature as function of clay content were performed at atmospheric pressure, the temperature dependent measurements, starting at −10 °C were performed under vacuum. The heating rate between the isothermal measurements was

1 °C/min. The time difference between the start gamma ray, emitted at the birth of the positron, and one of the stop gamma rays, emitted at the annihilation, was recorded employing a fast–fast coincidence system.

The spectra were evaluated using the POSITRONFIT [40] software, which fits the measured spectra with a model function consisting of a sum of decaying exponentials convoluted with the resolution function of the lifetime spectrometer plus a constant background. The resolution function was obtained from reference measurements on Kapton before the measurement series. The PALS measurements showed a rather broad distribution of *o*-Ps lifetimes in the organically modified clay. Due to this broadness, and the accompanying partial overlap of the lifetime distribution in the organically modified clay and the polyamide 6, it was not possible to resolve the *o*-Ps lifetime of the respective components in the composites. A three-component fit was, therefore, used when evaluating all the measured spectra. The shortest lifetime was fixed to 0.125 ns. Using a three-component fit, the *o*-Ps lifetime in PA6/clay composites will be a forced average of *o*-Ps lifetimes in the two phases, polymer and modified clay. In order to separate changes in *o*-Ps lifetime, due to the additive effect, from changes caused by actual free volume changes in the polymer and/or modified clay, lifetime spectra representing immiscible mixtures of PA6/modified clay nanocomposites were simulated. The simulated composite spectra were based on measured spectra of PA6 and organically modified clay, weighted with the respective weight fraction of the components. The simulated spectra, therefore, represent positron annihilation in PA6/clay composites with no changes in either matrix or modified clay structure due to mixing.

2.5. Dynamic mechanical analysis (DMA)

The shear storage (G') and loss modulus (G'') were determined, using an automated torsion pendulum ATM3 from Myrenne, during heating 2 °C/min starting from −100 to 200 °C at 1 Hz. The measurements were performed under a dry nitrogen atmosphere. The mechanical properties were measured on materials obtained after compression molding. In addition to previous treatment, the samples were again dried in vacuum at 80 °C for 24 h before measuring.

2.6. Small angle X-ray scattering (SAXS)

The inter-gallery spacing of layered silicates was studied with a Kratky compact camera equipped with a linear sensitive detector OED 50 M from MBraun. The Cu K_α radiation ($\lambda = 1.542$ Å) was generated with a Seifert ID 3000. The samples were placed in a sealed holder between mica sheets and were measured for 1 h at room temperature. The spacing (d) of the clay layers was determined from the angle (θ) of maximum scattering according to Bragg's relation: $\lambda = 2d \sin\theta$.

3. Results and discussion

Table 1 displays the inter-gallery spacing of the as received organically modified clays and PA6/clay nanocomposites with 4–35 wt% organically modified clay (Cloisite20A). The inter-gallery spacing of the clay in the composites is increased with 0.9–1.8 nm, as compared to the neat organically modified clay, showing that polymer chains have entered the clay galleries in all composites. Considering that the inter-gallery distance is only a fraction of the mean end to end distance of an unperturbed PA6 chain [41], the polymer chains present in the inter-gallery region experience significant one-dimensional confinement. A crude estimate, based on a purely intercalated composite without the presence of exfoliated platelets (Eq. (2)), suggests that about 11 wt% of the polymer can be present in the galleries in PA6/clay nanocomposite with 35 wt% clay.

$$w_i = \frac{SA w_s \Delta l \rho}{2(1 - w_c)} \tag{2}$$

SA refers to the specific surface area of the clay and is reported to be at least 750 m^2/g [35]. Δl is the increase of the inter-gallery distance upon mixing organically modified clay with PA6 (0.9 nm for PA6/clay nanocomposite with 35 wt% clay). ρ refers to the polymer density, taken as the measured bulk polymer density (1.018 g/cm^3) neglecting any differences in the inter-gallery region. W indicates the weight fraction of polymer in the inter-gallery region (i), silicate (s) and modified clay (c).

3.1. Thermal and dynamic mechanical properties

In Fig. 2(a), DSC heating scans of intercalated PA6/clay nanocomposites are shown. The melting of PA6 crystals occurs at temperatures between 190 and 250 °C. The melting of unfilled PA6 has two maxima at 212 and 222 °C, which corresponds well with reported melting temperatures of the γ- and α-form PA6 crystals, respectively [42], with the higher temperature endotherm (α) exhibiting the highest intensity. Upon addition of clay, the fraction of crystals melting close to 212 °C increases as compared to the fraction of α-form crystal, indicating an increasing fraction of γ-form crystals. An increased fraction of γ-form crystals in these PA6/clay nanocomposites with increasing clay content has earlier been noticed by means of temperature derivative FTIR measurements [14]. A third broad melting range close to 235 °C, indicating the presence of a crystal phase with increased stability, emerges upon clay addition and is observed in composites with 14–35 wt% clay content. This stable crystal phase has earlier been shown to consist of γ-form crystals [14]. Chain orientation, when stable at elevated temperatures ($T > T_g$), can lead to an increased melting temperature and in the case of PA6 also to favored formation of γ-crystals [42]. Chain deformation and

Table 1
Inter-gallery spacing of organically modified clays and PA6/Cloisite20A composites as measured with small-angle X-ray scattering

Inter-gallery spacing of organically modified clays (nm)					
Cloisite Na^+	Cloisite 20A	Cloisite 30B	Cloisite 93A		
1.17[a]	2.42[a], 2.4	1.85[a]	2.36[a]		
Inter-gallery spacing of PA6/Cloisite20A composites (nm)					
4 wt% clay	10 wt% clay	14 wt% clay	19 wt% clay	27 wt% clay	35 wt%
4.1	3.9	4.2	4.1	3.5	3.3

[a] Inter-gallery spacing obtained from the supplier [35]. The inter-gallery distance equals the inter-gallery spacing minus the thickness of the silicate layer (1.0 nm).

orientation can be caused by stresses created during extrusion of polymer clay nanocomposites due to high shear forces and interaction of polymer segments with the clay surface.

Fig. 2(b) shows that the fraction of crystals, which melt close to 212 and 235 °C is reduced upon repeated heating and cooling. Chain orientation, when introduced during processing of a non-crosslinked polymer, can be expected to be relieved upon melting of the crystals. The change in crystalline structure upon repeated heating and cooling, therefore, indicates that the formation of γ-form crystals and a more stable crystal phase in these PA6/clay nanocomposites is a combinatorial effect of thermal history and processing conditions in combination with the presence of clay particles. These results agree well with previous studies on the crystallinity in PA6/clay nanocomposites, which have shown γ-form crystals to be more stable in composites, where PA6 chains are tethered to the clay surface [11]. However, even after three repeated heating cycles a fraction of the crystals still exhibits increased stability and melt close to 235 °C. This indicates that some degree of chain orientation exhibits long-term stability, possibly stabilized by the presence of clay particles, in agreement with previous reports [7,11,14,43].

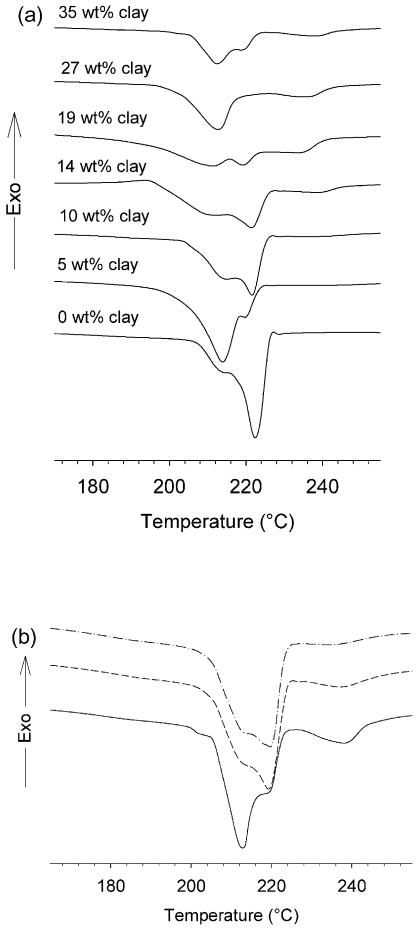

Fig. 2. (a) Heat flow from DSC heating scans of PA6/clay nanocomposites. (b) Heat flow from repeated DSC scans of PA6/clay nanocomposites with 35 wt% clay. The effect of repeated heating and cooling on PA6 with 35 wt% clay is representative for all measured PA6/clay nanocomposites. First heating (solid), second heating (dash) and third heating (dash-dot).

Fig. 3 displays the effect of clay on the heat of fusion (ΔH) of PA6 crystals and the change in heat capacity (ΔC_p) at the bulk glass transition in PA6/clay composites. The heat of fusion of PA6 is fairly constant up until 19 wt% clay, after which it decreased reaching a reduction of about 20%, as compared to unfilled PA6 at 35 wt% clay content. Considering that the heat of fusion of γ- and α-form crystals has been reported to be approximately equal, 239 and 241 J/g, respectively [44], the reduction of the heat of fusion in PA6/clay composites at high clay content (>19 wt%) does not appear to be due to different crystalline forms (γ and α). The

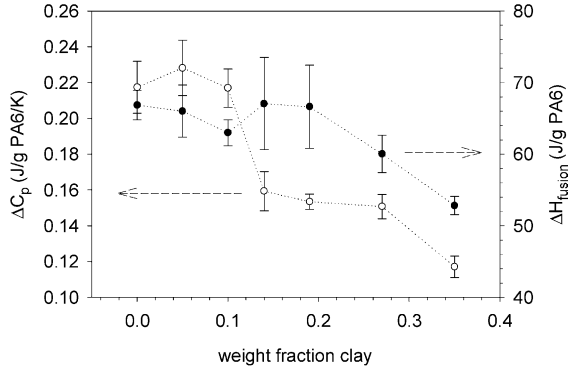

Fig. 3. Change in heat capacity (ΔC_p) of the polymer at the glass transition and the heat of fusion (ΔH) of the polymer as function of clay content in PA6/clay nanocomposites. ΔC_p of the polymer was measured between 45 and 75 °C. ΔC_p (empty circles) and ΔH (filled circles) in PA6/clay nanocomposite and unfilled polymer are normalized with reference to the polymer content.

reduced heat of fusion thus indicates that the degree of crystallinity of PA6 is decreased upon addition of high concentrations of clay. Due to the geometric constrictions it is unlikely that the fraction of polymer present between the clay layers, which is less than 11 wt% in PA6 with 35 wt% clay, is able to crystallize, which can account for part of the reduction in crystallinity [4]. In addition, it is possible that the presence of high concentrations of intercalated clay agglomerates and some exfoliated clay particles hinders the growth of crystalline lamellas, creating more amorphous defects in the crystalline regions, in agreement with previous reports [14].

ΔC_p at the glass transition, measured at around 56 °C in PA6, remains unaffected up until 10 wt% clay after which it is continuously decreasing reaching a reduction of close to 50% at 35 wt% clay. The observed reduction of ΔC_p for PA6 at the glass transition upon addition of clay would normally be accounted for by an increased crystallinity. However, as mentioned above, such an increase of the crystallinity was not observed in these PA6/clay nanocomposites. The reduction of ΔC_p, therefore, has to be interpreted as an altered mobility in the non-crystalline regions. This agrees well with the observed changes in crystalline morphology. In addition, the fraction of polymer present between clay layers, separated by about 1 nm, experiences an environment much different than the bulk polymer. Interaction with the organic modifier and/or silicate surfaces, as well as confinement in spaces smaller than the typical length-scale of cooperative motions, are likely to influence the mobility of polymers [3,45–47].

The loss shear (G'') modulus of PA6/clay composites at temperatures between −100 and 200 °C in Fig. 4(a) shows a significantly altered viscoelastic response of PA6/clay nanocomposites as compared to unfilled PA6. The mechanical losses increase in magnitude with increasing clay content with a maximum deviation from the behavior of unfilled PA6 around 0 and 120 °C, indicative of a broadening of the glass transition. Chain deformation and orientation, as was suggested to be the cause of the observed changes of the crystalline structure in PA6/modified clay nanocomposites, will effect the polymer mobility and hence also the glass transition behavior [46,48]. However, if chain deformation and orientation is localized to regions close to the clay surface, creating an interphase with properties different from the bulk phases, the mechanical losses do not necessarily reflect actual molecular relaxations in the interphase. The observed increased mechanical losses can be a micro-mechanical transition, a combinatorial effect of the morphology of the composite and the properties of the bulk phases and the interphase [49,50]. In such a case, the contribution from an interphase, composed of polymer segments and/or modifier, to the viscoelastic response of the nanocomposite would be enhanced. Fig. 4(a) also includes the shear loss modulus of PA6 with 7 wt% organic modifier, which displays a small loss peak at around 10 °C. In addition, at temperatures above the glass transition, the

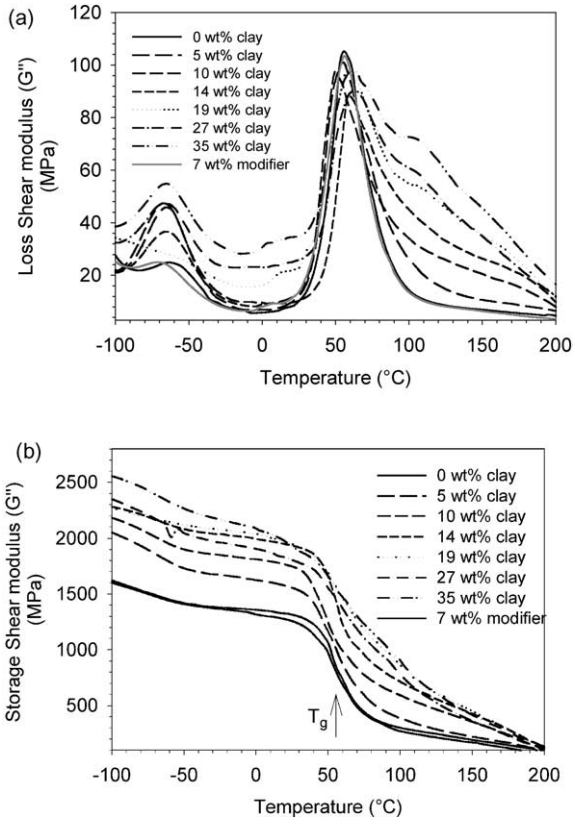

Fig. 4. (a) Shear Loss modulus of PA6/clay (G'') nanocomposites and PA6 mixed with 7 wt% organic modifier. (b) Shear Storage modulus of PA6/clay (G') nanocomposites and PA6 mixed with 7 wt% organic modifier.

mobility of the polymer can be sufficient to allow for crystalline rearrangements causing increased mechanical losses in this temperature region.

The storage shear modulus (G') of PA6/clay composites, shown in Fig. 4(b), increases with increasing clay content both above and below T_g. G' at −20 °C increases from about 1.4 GPa for unfilled PA6 to 2.2 GPa at 35 wt% clay content. The reinforcing effect of the clay is as expected larger at temperatures above T_g as compared to below T_g due to the decrease of the modulus of PA6 when passing from the glassy to the rubbery state. G' at 150 °C increases from about 0.2 GPa for unfilled PA6 to 0.4 GPa at 35 wt% clay content. It is, however, clear that the observed increase of the shear modulus in the intercalated PA6/clay nanocomposites is much lower than what is expected for nanocomposites with exfoliated clay particles [51,52].

3.2. Free volume sizes

DSC and DMA measurements showed a considerable effect of organically modified clay on the thermal and viscoelastic behavior of PA6, suggested to be caused by coil deformation and orientation in the composites and the significantly altered environment experienced by the polymer segments present between clay layers. Chain deformation and orientation, caused by internal stresses

[53–55] and interaction with surfaces [27,28,56] alter the free volume sizes in polymers. Measuring the free volume sizes in the PA6/clay nanocomposites can, therefore, provide further insight into the effect of clay on the behavior of polymers.

The measured and simulated free volume sizes in PA6/clay composites as a function of weight content clay is shown in Fig. 5. The corresponding measured *o*-Ps lifetimes and intensities are shown in Table 2. The simulated free volume cavity diameter represents the mean of a weight average of cavity sizes in a physical mixture of polymer and clay with no changes in the free volume sizes in either polymer or clay, i.e. the free volume structure of the respective components is not influenced by the presence of the other component. The simulation procedure is described in Section 2. The measured mean free volume cavity diameter in PA6/clay nanocomposites follows the simulated cavity diameter at clay concentrations up to 19 wt%. At high concentrations of clay (>19 wt%) an increase in the free volume cavity diameter is observed. At 35 wt% clay the measured mean free volume diameter is 0.55 nm, as compared to the simulated cavity diameter of 0.53 nm, indicating a lower chain packing efficiency in PA6/clay nanocomposites. Such a small increase in free volume size might appear insignificant, but it has been shown that seemingly small changes in free volume size have a large effect on the physical properties of polymers, such as bulk modulus and gas diffusion coefficients [54,57,58]. This sensitivity of the properties of polymers towards the free volume cavity size can be explained by the high concentration of free volume cavities ($\approx 10^{20}$/g) in polymers [59–61].

In addition, the measured mean free volume diameter is likely to be a weight average of the cavity sizes in the unaffected bulk and affected regions of the composite. The changes in free volume cavity size in affected regions can, therefore, be expected to be larger than the mean difference, which can be shown via a simplified estimation of the free volume sizes in the affected regions of the composite. The estimation (Eq. (3)) is based on linear weight addition of the *o*-Ps lifetime (τ_3) and intensity (I_3) in three phases, bulk polymer (p), organically modified clay (c), affected regions (i) and the measured *o*-Ps lifetime in the resulting nanocomposite (nc). *w* indicates the estimated weight fractions of the respective phases. Assuming that the effects on the free volume sizes are localized to a 1 nm thick polymer layer covering all of the clay surface, which roughly corresponds to 16 wt% of the nanocomposite, this estimation indicates that the *o*-Ps lifetime in the affected regions can then be increased to about 2.29 ns. The corresponding free volume size in the affected polymer phase, which is equal to about 0.62 nm is then much larger than the free volume size in the bulk PA6, which is equal to 0.51 nm.

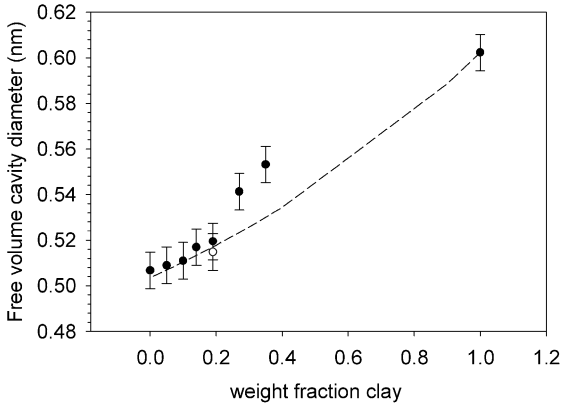

Fig. 5. Mean free volume cavity diameter in PA6/clay nanocomposites (●) as function of modified clay content and mean free volume cavity diameter in PA6 with 7 wt% organic modifier (○). The cavity diameter in PA6 mixed with modifier is displayed as 19 wt% modified clay, which corresponds to 7 wt% modifier. Simulated free volume cavity diameter in a physical mixture of PA6 and modified clay is depicted as a dashed line.

Table 2
ortho-Positronium lifetime and intensity in PA6/clay nanocomposites measured at ambient conditions

Clay content (wt%)	τ_3 (ns) ± 0.02	I_3 (%) ± 0.5
0	1.67	22.9
5	1.68	22.1
10	1.69	21.7
14	1.72	21.8
19	1.73	21.1
27	1.84	20.7
35	1.90	19.2
100	2.17	12.2

$$\tau_{3i} = \frac{\tau_{3nc}\left\lfloor I_{3p}(1-w_c) + I_{3c}w_c \right\rfloor - \left\lfloor \tau_{3p}I_{3p}(1-w_c-w_i) + \tau_{3c}I_{3c}w_c \right\rfloor}{I_{3p}w_i} \quad (3)$$

Although it is far from certain that free volume size changes are localized to a nano-meter thick polymer layer covering the clay surface, this estimation shows that large changes in affected regions of the composite can have a relatively small effect on the mean free volume size. It is, therefore, possible that while DSC and DMA experiments showed an altered behavior of the polymer/clay nanocomposites already at lower concentrations of clay (<27 wt%) the detection of altered free volume sizes at these filler contents is limited by the sensitivity of the PALS measurement. Fig. 5 also shows that addition of 7 wt% organic modifier to unfilled PA6 does not influence the mean free volume cavity diameter significantly.

The temperature dependence of the free volume diameter at temperatures between −10 and 150 °C in unfilled PA6, organically modified clay and intercalated PA6/clay nanocomposite containing 35 wt% clay is displayed in Fig. 6. Enclosed in Fig. 6 is also the inter-gallery spacing of the organically modified clay (Cloisite20A) obtained from Gelfer et al. [65]. The corresponding *o*-Ps lifetimes and intensities are displayed in Table 3. Around 60 °C a second

order transition of the temperature dependence of the free volume sizes in unfilled PA6, indicative of the glass transition, is observed. The glass transition of PA6, measured with DSC, was located at 56 °C. The mean free volume cavity size in glassy PA6 ranges from 0.47 to 0.50 nm and is increased to 0.62 nm at 150 °C, which is in good agreement with previous studies [62].

The mean free volume size in the modified clay, is increased from 0.54 nm at −10 °C to 0.65 nm at 70 °C. DSC heating scans displayed in Fig. 7 show that the organic modifier in the clay undergoes a transition with a maximum at around 47 °C. This transition corresponds to a phase transition from a well ordered structure with a low *gauche*/*trans* conformation ratio to a disordered liquid like structure with a high ratio of gauche conformations [63–65]. A liquid-like structure will have lower chain packing, which explains the increase in free volume size in this temperature region. The transition behavior of the organic modifier is sensitive to the environment in which the modifier is present, as evidenced by the shift from 59 to 47 °C when comparing free organic modifier and organic modifier exchanged with cations in the inter-gallery regions of the clay. The order to disorder transition is shifted to an even lower temperature of about 32 °C when the organically modified clay is mixed with PA6 forming intercalated PA6/clay nanocomposites. Above 70 °C the free volume sizes in the organic modifier in the clay decreases slightly to about 0.64 nm at 150 °C. This is rather surprising and indicates an intricate relationship between the free volume sizes in the organic modifier and inter-gallery spacing of the clay, which is increasing from 1.6 to 1.8 nm in the same temperature region. Contrary to what is observed it could be expected that the free volume sizes in the organic modifier should continuously increase above the order to disorder transition at 70 °C. The inverse relationship between the free volume sizes in the organic modifier and the inter-gallery spacing, at temperatures

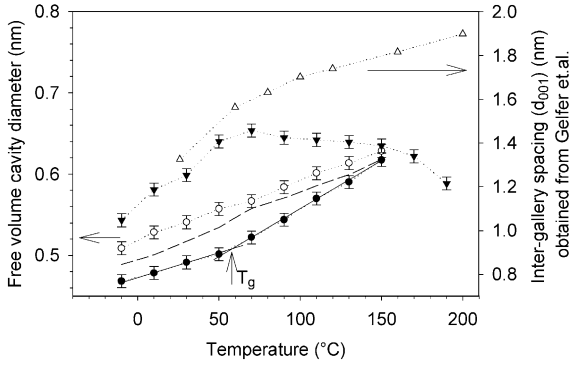

Fig. 6. Left axis: Mean free volume cavity diameter in PA6 (●), PA6/clay nanocomposites with 35 wt% clay (○), organically modified clay (▼) and simulated mean free volume cavity diameter in PA6/clay nanocomposites with 35 wt% clay (- - - -) as function of temperature between −10 and 190 °C. Right axis: Inter-gallery spacing (△) of the modified clay as function of temperature between 26 and 200 °C from Gelfer et al. [63]. Arrow indicates the glass transition temperature of PA6 measured with DSC and DMA.

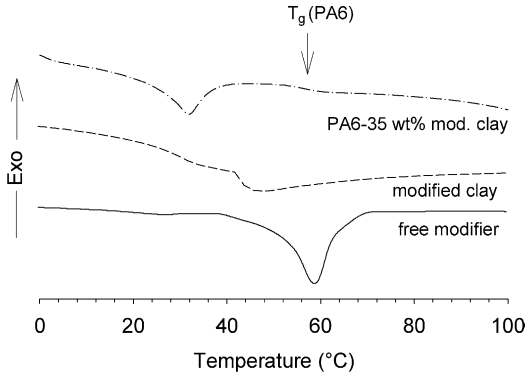

Fig. 7. DSC heating scans of free organic modifier (solid), organically modified clay (dash) and PA6 mixed with 35 wt% organically modified clay (dash-dot). The heating rate was 20 °C/min. Arrow indicates the glass transition of PA6.

above the order to disorder transition of the organic modifier, could be explained by excess organic modifier entering in the inter-gallery region when the molecular mobility is increased. An increasing number of aliphatic units per unit surface area of the clay, which can results in a larger inter-gallery spacing [63,66] can, however, also be accompanied by an increasingly ordered structure of the molecules due to the decrease in available volume to each molecule in the inter-gallery regions. The onset of degradation of the organic modification has been reported to occur at temperatures between 155 and 180 °C [65,67], which can explain the larger decrease of the free volume sizes with increasing temperature observed at temperatures above 150 °C.

The apparent intricate relationship between the free volume size and inter-gallery spacing of this organically modified clay, as evidenced by the shift of order-to disorder transitions upon intercalation and the inverted relationship between free volume size and inter-gallery spacing when measured above and below this transition, promotes an extension of this study to include additional modified clays. The free volume sizes and inter-gallery spacing of a number of clays, modified with different alkylammonium salts, are shown in Fig. 8. Although a weak trend of increasing free volume sizes with decreasing inter-gallery spacing appears to be present, it is also clear that such a comparison requires additional knowledge of the actual state of the modified clays. The number of aliphatic ions per unit surface area of the clay, the length of these chains and also the chain mobility, which is influenced by the temperature, will influence the free volume sizes as well as the correlation with the inter-gallery spacing [66].

The free volume sizes in PA6/clay composite with 35 wt% clay increases from 0.51 nm at −10 °C to 0.63 nm at 150 °C. The measured free volume sizes are larger than the simulated free volume sizes in the entire temperature range. DSC and DMA measurements have shown that the properties of the polymer in intercalated PA6/clay nanocomposites is significantly influenced by the modified clay.

Table 3
ortho-Positronium lifetime and intensity in unfilled PA6, organically modified clay and PA6/clay nanocomposite with 35 wt% modified clay at −10–190 °C

Temperature (°C)	PA6		Clay		PA6/clay	
	$\tau_3 \pm 0.02$ (ns)	$I_3 \pm 0.5$ (%)	$\tau_3 \pm 0.02$ (ns)	$I_3 \pm 0.5$ (%)	$\tau_3 \pm 0.02$ (ns)	$I_3 \pm 0.5$ (%)
−10	1.50	25.3	1.85	12.8	1.68	21.3
10	1.54	25.7	2.05	11.9	1.78	21.1
30	1.60	25.7	2.15	12.7	1.84	21.6
50	1.65	26.2	2.40	13.7	1.92	21.9
70	1.75	25.6	2.49	14.1	1.97	22.2
90	1.85	25.0	2.43	14.5	2.07	22.0
110	1.99	24.1	2.42	14.4	2.17	21.7
130	2.10	23.7	2.40	14.0	2.24	21.8
150	2.26	23.1	2.37	13.3	2.33	21.5
170	–	–	2.29	12.3	–	–
190	–	–	2.10	12.1	–	–

DSC measurements have shown that also the organic modifier is influenced by the presence of the polymer in the intercalated composites causing a shift of the order to disorder transition of the organic modifier from 47 to 32 °C (Fig. 7), when the organically modified clay is mixed with PA6. The shift of this transition will most likely cause a horizontal shift, along the temperature axis, of the free volume sizes in the organic modifier. According to simulated data, a shift of the order to disorder transition with 20 °C, which is 5 °C larger than what was measured with DSC, would increase the *o*-Ps lifetime in the intercalated PA6/nanocomposite to about 1.78 ns, corresponding to 0.53 nm, at 30 °C, without any effects on the polymer free volume sizes being present. When comparing this simulated lifetime and free volume diameter with the actual measured lifetime and corresponding diameter at 30 °C, 1.84 ns and 0.54 nm, respectively, it appears likely that the free volume sizes in both the organic modifier and the polymer are affected in these intercalated PA6/clay nanocomposites. Since mixing free organic modifier with PA6, without the presence of clay, did not result in any significant free volume changes (Fig. 5), it is possible that observed free volume changes in the intercalated PA6/clay nanocomposites are promoted by the clay layers.

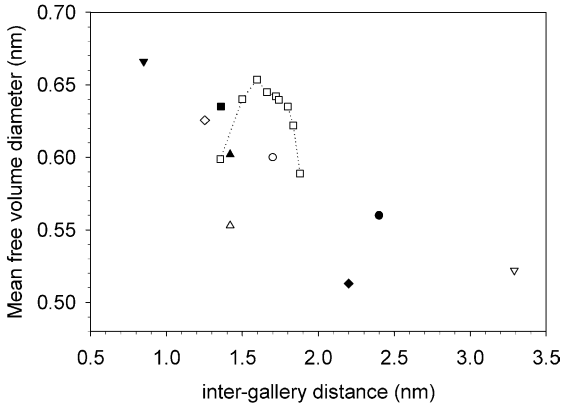

Fig. 8. Mean free volume cavity diameter in organically modified clay versus inter-gallery spacing. (▲) Montmorillonite modified with dimethyl, dihydrogenatedtallow, quaternary ammonium measured at ambient conditions. (■) Montmorillonite modified with methyl, dihydrogenatedtallow ammonium measured at ambient conditions. (▼) Montmorillonite modfied with methyl, tallow, bis-2-hydroxyethyl, quaternary ammonium cation measured at ambient conditions. (□) Montmorillonite modified with dimethyl, dihydrogenatedtallow, quaternary ammonium measured at temperatures between 30 and 190 °C, inter-gallery spacing (d_{001}) [65]. (○, ●) Montmorillonite modified with long-chain alkylammonium cations measured at ambient condition [68]. (◇) Organically modified mica-type silicate measured at ambient condition [31]. (◆) Montmorillonite modified with octadecylammonium cation [69]. (▽) Rectorite modified with octadecylammonium cation [33]. (△) Montmorillonite modified with octadecylammonium cation measured at ambient condition [32].

4. Conclusions

High concentrations of organically modified clay dispersed in a PA6 matrix was found to significantly influence the thermal and viscoelastic behavior of the polymer. The clay promoted an increased fraction of γ-form crystals and the appearance of an additional crystal phase with increased thermal stability. A decreased heat of fusion of PA6, at high clay contents (>19 wt% clay), indicating a significant decrease in the degree of crystallinity of the polymer, as well as a decrease of the ΔC_p at the glass transition of the bulk polymer was measured. These rather conflicting findings were interpreted as an altered mobility in the non-crystalline regions. A broadening of the glass transition upon addition of modified clay was also observed by means dynamic mechanical analysis. PALS measurements showed that high concentrations of clay (>19 wt%) caused an increase of the mean free volume cavity diameter in the composites, suggesting a lower chain packing efficiency in the intercalated PA6/clay nanocomposites. The lower packing efficiency was observed both above and below the glass transition of the polymer. However, not only was the polymer affected by the presence of the clay, but also the behavior of the organic modifier, which constituted a significant fraction of these nanocomposites, was influenced by the presence of both clay and polymer. The order to disorder transition of the organic modifier, when

exchanged with cations between the clay layers, was shifted with 12 °C towards lower temperatures, as compared to the free organic modifier. The transition was shifted to even lower temperatures when the organically modified clay was dispersed in the PA6 forming intercalated polymer nanocomposites. It is, therefore, likely that the measured increase of free volume sizes in the nanocomposites originates from structural changes in both the polymer as well as the organic modifier. The changes found in the behavior of the organic modifier in combination with the large effects that the clay was shown to have on the crystalline structure of the polymer, makes the process of deducing a quantitative measure of the effect of organically modified clay on the free volume sizes in PA6 challenging.

Acknowledgements

The authors would like to thank John Algers for valuable discussions. Jens Norrman and Katarina Flodström at the department of Physical Chemistry, Lund University is acknowledged for the help with the SAXS measurements. This work was supported by the Swedish Research Council. DSM, the Netherlands, is acknowledged for providing the samples.

References

[1] Anastasiadis SH, Karatasos K, Vlachos G, Manias E, Giannelis EP. Phys Rev Lett 2000;84(5):915–8.
[2] Giannelis EP. Adv Mater 1996;8(1):29–35.
[3] Giannelis EP, Krishnamoorti R, Manias E. Adv Polym Sci 1999;138: 107–47.
[4] Vaia RA, Sauer BB, Tse OK, Giannelis EP. J Polym Sci, Part B: Polym Phys 1997;35(1):59–67.
[5] Lu HB, Nutt S. Macromolecules 2003;36(11):4010–6.
[6] Hu XS, Zhang WH, Si MY, Gelfer M, Hsiao B, Rafailovich M, et al. Macromolecules 2003;36(3):823–9.
[7] Kojima Y, Matsuoka T, Takahashi H, Kurauchi T. J Appl Polym Sci 1994;51(4):683–7.
[8] Kojima Y, Usuki A, Kawasumi M, Okada A, Kurauchi T, Kamigaito O, et al. J Polym Sci, Part B: Polym Phys 1995;33(7): 1039–45.
[9] Jimenez G, Ogata N, Kawai H, Ogihara T. J Appl Polym Sci 1997; 64(11):2211–20.
[10] Mathias LJ, Davis RD, Jarrett WL. Macromolecules 1999;32(23): 7958–60.
[11] Lincoln DM, Vaia RA, Wang ZG, Hsiao BS, Krishnamoorti R. Polymer 2001;42(25):9975–85.
[12] Liu XH, Wu QJ, Berglund LA. Polymer 2002;43(18):4967–72.
[13] Liu XH, Wu QJ, Zhang QX, Berglund LA, Mo ZS. Polym Bull 2002; 48(4/5):381–7.
[14] van Es M. PhD Thesis, Technische Universiteit Delft, Delft; 2001.
[15] Wu HD, Tseng CR, Chang FC. Macromolecules 2001;34(9):2992–9.
[16] Nam JY, Ray SS, Okamoto M. Macromolecules 2003;36(19): 7126–31.
[17] Fornes TD, Paul DR. Polymer 2003;44(14):3945–61.
[18] Krishnamoorti R, Vaia RA, Giannelis EP. Chem Mater 1996;8(8): 1728–34.
[19] Swenson J, Howells WS. J Chem Phys 2002;117(2):857–65.
[20] Manias E, Kuppa V. Eur Phys J E 2002;8(2):193–9.
[21] Beuche F. Physical properties of polymers. New York: Wiley; 1962.
[22] Ferry JD. Viscoelastic properties of polymers. New York: Wiley; 1980.
[23] Algers J, Suzuki R, Ohdaira T, Maurer FHJ. Macromolecules 2004; 37(11):4201–10.
[24] Algers J, Suzuki R, Ohdaira T, Maurer FHJ. Polymer 2004;45(13): 4533–9.
[25] Jean YC, Zhang RW, Cao H, Yuan JP, Huang CM, Nielsen B, et al. Phys Rev B 1997;56(14):R8459–R62.
[26] He C, Hamada E, Suzuki T, Kobayashi H, Kondo K, Shantarovich VP, et al. J Radioanal Nucl Chem 2003;255(3):431–5.
[27] Merkel TC, Freeman BD, Spontak RJ, He Z, Pinnau I, Meakin P, et al. Chem Mater 2003;15(1):109–23.
[28] Winberg P, Eldrup M, Maurer FHJ. Polymer 2004;45(24):8253–64.
[29] Merkel TC, He ZJ, Pinnau I, Freeman BD, Meakin P, Hill AJ. Macromolecules 2003;36(18):6844–55.
[30] Uedono A, Fukui S, Muramatsu M, Ubukata T, Kimura S, Tanigawa S. J Polym Sci, Part B: Polym Phys 2001;39(8):835–42.
[31] Olson BG, Peng ZL, Srithawatpong R, McGervey JD, Ishida H, Jamieson AM, et al. Mater Sci Forum 1997;255–257:336–8.
[32] Becker O, Cheng YB, Varley RJ, Simon GP. Macromolecules 2003; 36(5):1616–25.
[33] Wang SJ, Zhang M, Liu LM, Fang PF, Zhang SP, Wang B. Mater Sci Forum 2004;445–446:355–7.
[34] Wang YQ, Wu YP, Zhang HF, Zhang LQ, Wang B, Wang ZF. Macromol Rapid Commun 2004;25(23):1973–8.
[35] Product information from Southern Clay Products. Inc, USA.
[36] Mogensen O. Positron annihilation in chemistry. Berlin: Springer; 1995.
[37] Tao SJ. J Chem Phys 1972;56(11):5499.
[38] Eldrup M, Lightbody D, Sherwood JN. Chem Phys 1981;63(1/2): 51–8.
[39] Nakanishi H, Yean YC. Positron and positronium chemistry. Amsterdam: Elsevier; 1988 (chapter 5).
[40] Kirkegaard P, Pedersen N, Eldrup M. Risø-M-2740, Risoe National Laboratory; 1989.
[41] Brandrup J, Immergut EH, Grulke EA, editors. Polymer handbook. New York: Wiley; 1999. p. 63.
[42] Wunderlich B. Crystal melting. Troy, New York: Academic Press; 1980 (chapter 9).
[43] Liu TX, Liu ZH, Ma KX, Shen L, Zeng KY, He CB. Comp Sci Tech 2003;63(3/4):331–7.
[44] Illers KH. Makromol Chem-Macromol Chem Phys 1978;179(2): 497–507.
[45] Ngai KL. J Phys-Cond Matter 1999;11(10A):A119–A30.
[46] Yim St A, Pierre LE. Polym Lett 1969;7:237–9.
[47] Kirst KU, Kremer F, Litvinov VM. Macromolecules 1993;26(5): 975–80.
[48] Booij HC. Br Polym J 1977;9(1):47–55.
[49] Colombini D, Maurer FHJ. Macromolecules 2002;35(15):5891–902.
[50] Eklind H, Maurer FHJ. Polymer 1996;37(13):2641–51.
[51] Loyens W, Jannasch P, Maurer FHJ. Polymer 2005;46(3):903–14.
[52] Deanin RD, Schott NR. Fillers and reinforcements for plastics. Washington, DC: American Chemical Society; 1974.
[53] Schmidt M, Olsson M, Maurer FHJ. J Chem Phys 2000;112(24): 11095–106.
[54] Schmidt M, Maurer FHJ. Macromolecules 2000;33(10):3879–91.
[55] Dlubek G, Lupke T, Fretwell HM, Alam MA, Wutzler A, Radusch HJ. Acta Polym 1998;49(5):236–43.
[56] Merkel TC, Freeman BD, Spontak RJ, He Z, Pinnau I, Meakin P, et al. Science 2002;296(5567):519–22.
[57] Schmidt D, Shah D, Giannelis EP. Curr Opin Solid State Mater Sci 2002;6(3):205–12.
[58] Nagel C, Gunther-Schade K, Fritsch D, Strunskus T, Faupel F. Macromolecules 2002;35(6):2071–7.

[59] Jordan SS, Koros WJ. Macromolecules 1995;28(7):2228–35.
[60] Srithawatpong R, Peng ZL, Olson BG, Jamieson AM, Simha R, McGervey JD, et al. J Polym Sci, Part B: Polym Phys 1999;37(19): 2754–70.
[61] Dlubek G, Stejny J, Alam MA. Macromolecules 1998;31(14): 4574–80.
[62] Dlubek G, Redmann F, Krause-Rehberg R. J Appl Polym Sci 2002; 84(2):244–55.
[63] Vaia RA, Teukolsky RK, Giannelis EP. Chem Mater 1994;6(7): 1017–22.
[64] Okahata Y, Shimizu A. Langmuir 1989;5(4):954–9.
[65] Gelfer M, Burger C, Fadeev A, Sics I, Chu B, Hsiao BS, et al. Langmuir 2004;20(9):3746–58.
[66] Lagaly G. Solid State Ionics 1986;22:43–51.
[67] Xie W, Gao ZM, Pan WP, Hunter D, Singh A, Vaia R. Chem Mater 2001;13(9):2979–90.
[68] Consolati G, Natali-Sora I, Pelosato R, Quasso F. J Appl Phys 2002; 91(4):1928–32.
[69] Murakami H, Sano M, Hashimoto S. Mater Sci Forum 1997;255–257: 330–2.